Dispersive Diffraction in a Two-Dimensional Hexagonal Transmission Lattice

B. Osting[1], #H. S. Bhat[2]
[1]Columbia University
500 W. 120th St., New York, NY 10027, USA, bro2103@columbia.edu
[2]University of California, Merced
P. O. Box 2039, Merced, CA 95344, USA, hbhat@ucmerced.edu

1 Introduction

Consider a hexagonal LC lattice of inductors and capacitors. For the lattice diagram shown in Fig. 1, we assume that each edge consists of an inductor that connects two nodes, and that there is a capacitor connecting each node to a ground plane that is not pictured. This medium is a two-dimensional generalization of the standard transmission line structure. We take the inductances L and capacitances C to be identical at each edge and node. We assume the lattice is divided into two halves by a barrier with a thin slit. Waves of lattice voltage incident on this aperture will diffract. In this work, we seek to understand the effect that dispersion will have on the observed diffraction patterns, especially at wavelengths close to the Bragg cutoff for the lattice.

We are interested in this problem mainly because the lattice serves as a useful model for many two-dimensional, linear, dispersive media. The numerical solution of high-frequency diffraction problems in such media involves a computational discretization of the domain. For sufficiently high frequencies, waves propagating through the discrete domain will have wavelength comparable to the lattice spacing, at which point dispersive effects will be prominent. A full understanding of the influence of dispersion on diffraction in discrete domains is important for further advancement of high-frequency computational methods.

Additionally, we note that this work extends prior work that has analyzed diffraction in a square LC lattice while ignoring the effects of dispersion [1].

2 Derivation of the Diffraction Formula

Using the labeling of voltage nodes shown in Fig. 1, we use Kirchhoff's Laws to derive the following second-order equation for lattice voltage:

$$LC\frac{d^2}{dt^2}V_{i,j} = V_{i-1/2,j+1} + V_{i+1/2,j+1} + V_{i-1,j} + V_{i+1,j} + V_{i-1/2,j-1} + V_{i+1/2,j-1} - 6V_{i,j} \qquad (1)$$

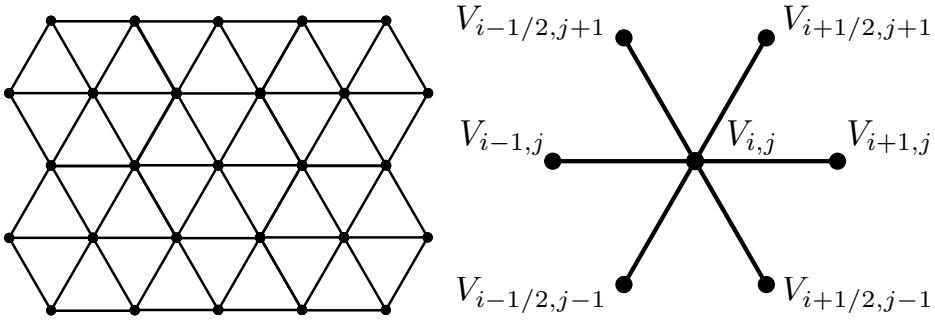

Figure 1: Regular hexagonal lattice

To analyze diffraction governed by this model, we derive a continuum PDE. Assume that each edge in the lattice has length $h > 0$. Define distributed inductance and capacitance given by $\ell = L/h$ and $c = C/h$. Let $V(x,y,t)$ denote the continuum approximation of $V_{i,j}(t)$ when $x = ih$ and $y = jh$. Then the Taylor expansion of the right-hand side of (1) about the central voltage $V_{i,j}(t)$ gives

$$\ell c\ddot{V} = \frac{3}{2}\nabla^2 V + \frac{3}{32}h^2\nabla^2\nabla^2 V + O(h^4). \tag{2}$$

Here overdots denote time derivatives and $\nabla^2 = \frac{\partial^2}{\partial x^2} + \frac{\partial^2}{\partial y^2}$ is the two-dimensional Laplacian. Note that (2) is the classical wave equation plus an $O(h^2)$ dispersive correction. Ignoring the $O(h^4)$ error term, we rearrange (2) to read $\nabla^2 V = \frac{2}{3}\ell c V_{tt} - \frac{1}{16}h^2\nabla^4 V$. Taking the Laplacian of both sides gives

$$\nabla^2\nabla^2 V = \frac{2}{3}\ell c\nabla^2 V_{tt} - \frac{1}{16}h^2\nabla^2\nabla^2\nabla^2 V.$$

Substituting this expression in (2), we obtain, after again truncating the $O(h^4)$ error term,

$$\ell c\ddot{V} = \frac{3}{2}\nabla^2 V + \frac{\ell c}{16}h^2\nabla^2\ddot{V} \tag{3}$$

The reason we have replaced (2) by (3) is that (2) has an unphysical blow-up at short wavelengths, while (3) does not. One may verify that the dispersion relation of (3) approximates the dispersion relation of the fully discrete equation (1) with an $O(h^4)$ error.

Substituting $V(x,y,t) = e^{\imath\omega t}U(x,y)$ into (3), we obtain the Helmholtz equation

$$\left(\nabla^2 + \gamma_h^2\right)U = 0, \qquad \gamma_h^2 = \frac{16\ell c\omega^2}{24 - \ell c h^2\omega^2}. \tag{4}$$

Using standard techniques [2, 3], we may then derive from (4) the dispersively corrected two-dimensional Rayleigh-Sommerfeld (RS) diffraction integral

$$U(x,y) = -\frac{\gamma_h x}{2\imath}\int_{-\sigma}^{\sigma} U(\xi)\frac{H_1(\gamma_h|\mathbf{r}|)}{|\mathbf{r}|}d\xi. \tag{5}$$

Here the aperture is modeled by the interval $-\sigma \le \xi \le \sigma$ on the line $x = 0$. The quantity $|\mathbf{r}|$ stands for the magnitude of the vector $\mathbf{r}$ joining the point (x,y) to the point $(0,\xi)$ on the aperture. Equation (5) with γ_h replaced by $\gamma_0 = \sqrt{(2/3)\ell c\omega}$ is the traditional, non-dispersively corrected diffraction integral. Note that if γ_0 and h are both known, one can compute γ_h using $\gamma_h^{-2} = \gamma_0^{-2} - h^2/16$.

3 A Comparison of Diffraction Integrals

In this section, we quantify the effect of dispersion on observed diffraction patterns. In other words, we investigate how the RS integral (5) changes when we use γ_h given by (4) instead of the non-dispersive quantity $\gamma_0 = (2/3)\ell c\omega^2$. First we take a 640×640 lattice with a 4 node aperture centered along the left boundary. We set $h = 1/32$ and let $h\gamma_0 = \pi$ so that the effective wavelength is $\lambda_r = 2h$, close to the Bragg cutoff wavelength of $\sqrt{2}h$. We choose a constant input signal $U(\xi) = 1$ on the aperture. With these parameters, we evaluate (5) numerically, using both the dispersive γ_h and the non-dispersive γ_0.

Fig. 2 shows the intensity $|U|$ of the resulting non-dispersive and dispersive diffraction patterns. As shown, the net effect of dispersion is to compress the output in the y-direction. For example, it is evident that the non-dispersive pattern has three fringes, while the dispersive pattern has five. Though this result is for the constant input, extensive numerical tests have shown that if we choose

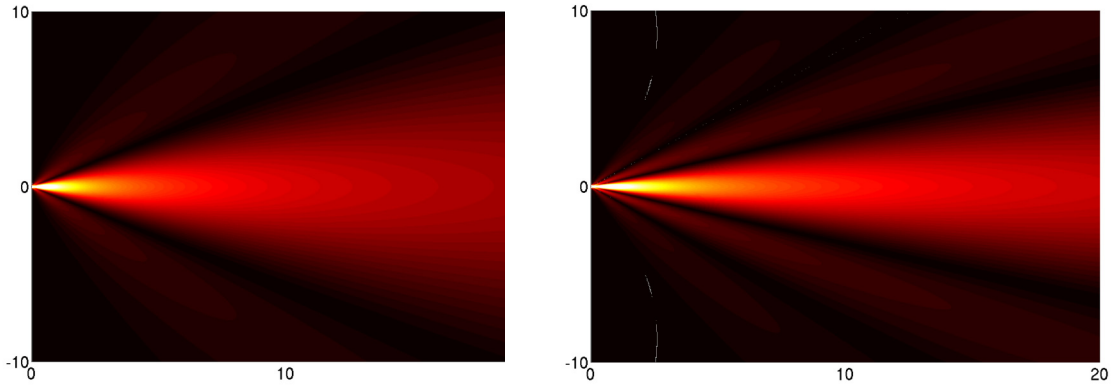

Figure 2: Comparison of traditional (left) and dispersively corrected (right) diffraction patterns, produced via numerical evaluation of (5) using γ_0 and γ_h, respectively. Note that dispersion changes the width and number of fringes in the diffraction pattern.

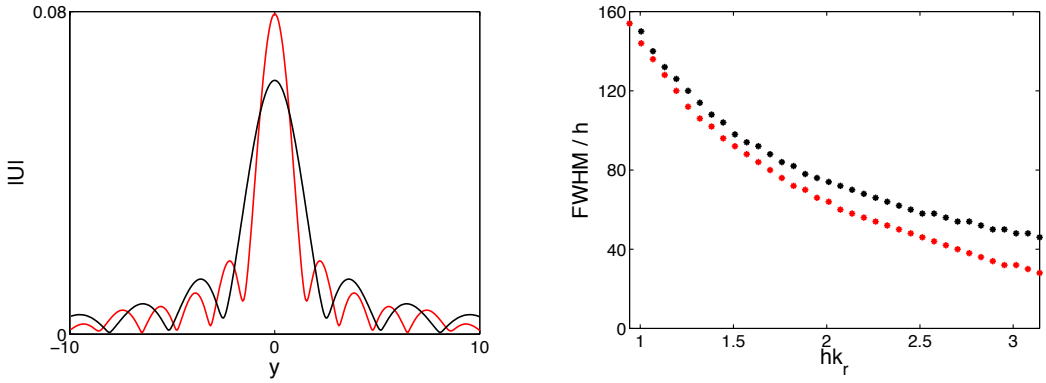

Figure 3: All plots are for a 320×320 lattice with a 16-node aperture and lattice spacing $h = 1/16$. On the left, we fix $h\gamma_0 = \pi$ and compute the dispersively corrected (red) and traditional (black) diffracted images at the far right of the domain. On the right, we show the full widths at half maximum (FWHM) of the central peak for dispersively corrected (red) and traditional (black) diffracted images, as the parameter $h\gamma_0 = hk_r$ is varied.

a Gaussian, sinusoidal or other type of input, as long as $h\gamma_0 = \pi$, the qualitative effect of the dispersive correction is the same: the diffracted output is compressed in the y direction.

For subsequent tests, we compute the output only along the right boundary of the domain. Consider first a 320×320 lattice with spacing $h = 1/16$ and an aperture width of 16 nodes. Again choosing a constant input signal $U(\xi) = 1$ on the aperture, we compute the traditional and dispersively corrected diffracted outputs at $h\gamma_0 = \pi$—see the left panel of Fig. 3. For the right panel of Fig. 3, we sweep through values of $h\gamma_0$ and compute the full width at half max (FWHM) of the central peak for both types of diffracted outputs. The FWHM difference for $h\gamma_0 = \pi$ is $18h$, a substantial difference considering that the aperture width is only $16h$.

The results so far might lead one to believe that the effect of dispersion is important *only* when $h\gamma_0 = \pi$, i.e., only when the effective wavelength is quite close to the Bragg cutoff. Our numerical tests have shown that this is true in the case when the input is a square wave. For our next test, we take a non-square wave input, e.g.,

$$U(\xi) = \begin{cases} (1/10)\sin^2(10\pi\xi) & \xi \in \Sigma \\ 0 & \xi \notin \Sigma. \end{cases} \tag{6}$$

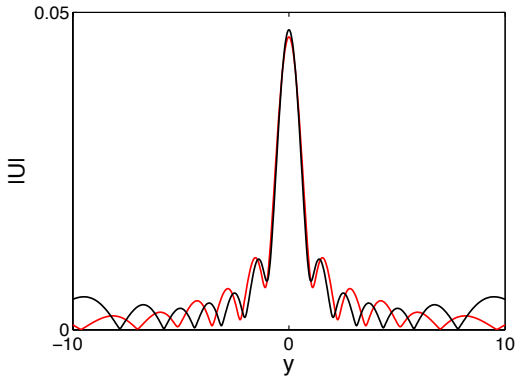

Figure 4: Traditional (black) and dispersively corrected (red) diffraction patterns at $h\gamma_0 = \pi/2$ for sinusoidal input given by (6). The output is taken at the right-hand side of a 280×640 lattice with spacing $h = 1/32$ and an aperture width of 32 nodes. Note that away from the central peak, the peaks of the red curve correspond to the zeros of the black curve.

We set $h = 1/32$ and use an aperture width of 32 nodes on a 280×640 lattice. In this case, even when $h\gamma_0 = \pi/2$, the dispersive and non-dispersive diffraction patterns are significantly different in the tails. As shown in Fig. 4, the peaks of the red (dispersive) signal correspond to the zeros of the black (non-dispersive) signal. This is true even though the FWHM values for the two signals are indistinguishable.

4 Conclusion

By deriving a PDE model for lattice voltage dynamics that tracks the dispersive correction to $O(h^2)$, we derived the dispersively corrected RS integral (5). Numerical experiments have confirmed that, when the effective wavelength is close to the Bragg cutoff, the dispersion of the medium causes a significant distortion in observed diffraction patterns: peak amplitudes, FWHM values, and fringe widths are all affected. Based on Fig. 4, we conjecture that for smaller values of $h\gamma_0$, there exist oscillatory input signals whose tail diffraction patterns can be substantially altered due to dispersion.

Acknowledgments

B. Osting is partially supported by the U.S. National Science Foundation (NSF), through the NYU-Columbia Research and Training Grant on Numerical Mathematics and Scientific Computing. H. S. Bhat is partially supported by NSF Grant No. DMS-07-53983.

References

[1] E. Afshari, H. S. Bhat, and A. Hajimiri, "Ultrafast analog Fourier transform using two-dimensional LC lattice," *IEEE Trans. Circ. Sys. I*, 2008, in press.

[2] C. J. Bouwkamp, "Diffraction Theory," *Rep. Prog. Phys.*, vol. 17, pp. 35–100, 1954.

[3] M. Born and E. Wolf, *Principles of Optics*, 6th ed. Pergamon Press, 1980.